PERGAMON

International Journal of Heat and Mass Transfer 44 (2001) 2311–2322

International Journal of HEAT and MASS TRANSFER

www.elsevier.com/locate/ijhmt

Natural convection from a vertical flat plate with a surface temperature oscillation

Jian Li [a,*], D.B. Ingham [b], I. Pop [c]

[a] *State Key Laboratory of Scientific and Engineering Computing, Institute of Computational Mathematics and Scientific/Engineering Computing, Chinese Academy of Sciences, Beijing 100080, People's Republic of China*

[b] *Department of Applied Mathematics, University of Leeds, Leeds LS2 9JT, UK*

[c] *Faculty of Mathematics, University of Cluj, R-3400 Cluj, CP 253, Romania*

Received 10 July 2000

Abstract

In this paper, we develop numerical methods for the natural convection flow from a vertical flat plate with a surface temperature oscillation. In the steady case, numerical results for the Grashof numbers 0–625 are obtained using an iterative approach and the results for small Grashof numbers are validated using a perturbation method. For larger values of the Grashof numbers, an unsteady numerical scheme is constructed and the results obtained at large times are compared with the steady solutions. Further, the results for very large Grashof numbers, up to 10 000, show that the unsteady solution approaches a steady solution. All the results obtained show that the proposed methods are very efficient and accurate.

1. Introduction

A body whose temperature is maintained at a higher value than that of the surrounding ambient fluid supplies heat to the medium and this results in the production of buoyancy forces within the medium. In a fluid of very small viscosity then boundary layers often exist and a classical example of such a flow is that of the fluid flow along a heated semi-infinite vertical flat plate, first considered by Pohlhausen [1], where the buoyancy force is parallel to the plate. This problem has become a very attractive and important subject of investigation over the last seven decades. A detailed review on the work of this famous problem has been given in several excellent review papers and books, see for example [2–8].

With the exception of a few specially prescribed boundary conditions at the wall, discovered by Sparrow and Gregg [9] and Semenov [10], the problem of vertical free convection boundary-layer flow is, in general, non-similar. Thus, one often has to solve a set of coupled nonlinear partial differential equations numerically. The local similar method avoids this by deleting the streamwise derivative terms and this changes the partial differential equations into nonlinear ordinary differential equations which still have to be solved numerically. However, the error introduced by this technique cannot be easily estimated and Sparrow et al. [11] introduced the locally non-similar method to improve this concept. However, like the locally similar method, this technique is locally autonomous. Solutions at any specified streamwise station can be obtained without first obtaining upstream solutions. Keller and Yang [12] employed a Gortler-type series to study the free convection boundary-layer over a non-isothermal vertical plate and in their analysis the wall temperature was assumed to be represented by a power series in the streamwise coordinate. Later, Kao et al. [13] proposed the method of strained coordinates for the computation of the wall heat transfer parameter for a plate with an arbitrary prescribed surface temperature. In this method, the coordinate along the plate was transformed by using an integral function of the specified wall temperature so that the problem can be solved once and for all with any specified surface conditions. The non-similar solution can then be obtained for the local similarity solution by

* Corresponding author.

E-mail addresses: lij@lsec.cc.ac.cn (J. Li), popi@math.ubbcluj.ra (I. Pop).

0017-9310/01/$ - see front matter
PII: S0017-9310(00)00276-3

Nomenclature

c, d	constants
g	magnitude of the gravitational acceleration
Gr	Grashof number $= g\beta\Delta T l^3/v^2$
l	length scaling
$\overline{Nu}$	average Nusselt number $= -\int_0^{\pi} \partial T/\partial y|_{y=0}\,\mathrm{d}x$
Pr	Prandtl number $= v/\alpha$
t	time
$T, \tilde{T}$	dimensionless temperatures defined in Eqs. (2) and (8)
u, v	dimensionless x- and y-velocity components
U_0	velocity scaling
x, y	Cartesian coordinates along and normal to the plate, respectively

Greek symbols

α	thermal diffusivity
β	coefficient of thermal expansion
γ	constant
Δt	time step
ΔT	temperature scaling
v	viscosity of fluid
$\psi, \tilde{\psi}$	dimensionless stream functions defined in Eqs. (2) and (8)
$\omega, \tilde{\omega}$	dimensionless vorticities defined in Eqs. (2) and (8)

Subscripts

w	condition at the wall
∞	ambient condition

Superscripts

$-$	dimensional variables
$'$	differentiation with respect to y

determining an appropriate wedge parameter in such a way that the local similarity results give a value that would be obtained if one considers the non-local similarity solution method. Following this technique, the determination of the appropriate wedge parameter involves an estimation and iterative procedure. Further, Yang et al. [14] proposed an alternative method to evaluate the surface heat transfer rate and the wall shear stress for this vertical free convection boundary-layer flow considered by Kao et al. [13] using a Merk-type series solution [15]. The governing coupled partial differential equations were transformed into a sequence of coupled ordinary differential equations which were then solved numerically by a fourth-order Runge–Kutta scheme with an incorporated least-squares convergence criteria for the zeroth-order solution and with the Newton–Raphson iteration scheme for higher-order solutions. Tables of the universal functions and their surface derivatives have been presented for some values of the Prandtl number. It is important to mention here the excellent paper by Na [16] in which a very efficient implicit finite-difference method, known as the Keller-box method and introduced by Keller and Cebeci [17], for more details see [18], has been used to solve the parabolic system of equations for the vertical free convection boundary-layer for a plate with non-uniform temperature distributions. Using this method, the resulting nonlinear difference equations are linearized by the method of quasilinearization and the algebraic equations are then solved by an efficient block-tridiagonal factorization technique. The local rates of heat transfer as a function of the distance along the plate were tabulated for a large range of values of the Prandtl number from 0.01 to 100 and for a few cases of the wall temperature distributions. It is worth mentioning that the Keller-box method has become a very popular technique in fluid mechanics and heat transfer theory, see for example [8,19].

The problem when the surface temperature on the vertical plate oscillates with the streamwise coordinate has been investigated by Yang [14], Na [16], Kao [20] and Rees [21]. However, very recently Rees [21] has studied, both numerically and analytically, the situation when the sinusoidal surface temperature oscillates about a constant mean value which is held above the ambient temperature of the fluid. The Keller-box method, coupled with a multi-dimensional Newton–Raphson iteration scheme was employed to solve the resulting set of nonlinear differential equations. In this methodology the difference equations are defined within the Fortran code and the iteration matrix, which is the Frechet derivative of the difference equations, has been determined using numerical differentiation, rather than being specified explicitly within the code. Such a technique, proposed by Rees [21], although slower in execution than when the matrix is defined explicitly, admits a much faster code development. Rees [21] has also made an asymptotic analysis which is valid at large distances from the leading edge. It was shown that an important feature of the flow is that a near-wall layer (inner layer) develops at large distances downstream of the leading edge and the growth of this inner layer decreases with increasing distance downstream. This observation is supported by both numerical simulations and the two-term asymptotic solution which are in extremely good agreement.

In spite of the extensive studies on the convective heat transfer from a heated vertical flat plate there is still a need for a more detailed solution method and accurate results of the governing coupled partial

differential equations, especially for surfaces with particular wall temperature distributions. Therefore the aim of this paper is to present a detailed study and to obtain very accurate results for the problem of free convection flow from a vertical flat plate whose surface temperature profile oscillates with the distance along the plate. The problem is studied using the full coupled momentum, vorticity and energy equations written in terms of the non-dimensional stream function, vorticity and temperature. This type of surface temperature distribution may be taken to model the effects of a periodic array of heaters behind or within the wall, see [21]. Although an accurate analysis of such a configuration would require a detailed examination of the effects of conduction within the heated wall, known as the conjugate problem, we simplify the problem by imposing a sinusoidal surface temperature distribution and we determine some information about the resulting flow and heat transfer characteristics using both numerical and series solutions. Both steady and unsteady formulations are investigated. For the steady-state case a series solution in powers of small Grashof number Gr is obtained and closed form analytical solutions, up to terms which are $O(Gr^2)$, are given for arbitrary Prandtl number Pr. The numerical methods for both the solution of the steady and the unsteady flow cases are then obtained assuming that the stream function, vorticity and temperature can be expressed in the form of a Fourier series expansion. In order to overcome the lack of detail on the vorticity on the boundary, we extend the method proposed by Li [22]. This method is different from the one which uses the vorticity integral condition which was first proposed by Dennis and Chang [23] and Collins and Dennis [24]. Numerical results have been obtained for a range of values of the Prandtl number but, for brevity, the results are only presented for $Pr = 1$.

Finally, it is worth mentioning that an analogous problem has been considered for a fluid-saturated porous medium by Poulikakos and Bejan [25], Bradean et al. [26–28] and Rees [29].

2. Governing equations

We consider the natural convection flow of a viscous and incompressible fluid over a vertical flat plate whose temperature $\bar{T}_w(\bar{x})$ oscillates with the streamwise coordinate $\bar{x}$ as follows:

$$\bar{T}_w(\bar{x}) = T_\infty + \Delta T \sin(\bar{x}/l), \tag{1}$$

where T_∞ is the temperature of the ambient fluid and l and ΔT are the typical length and temperature scales, respectively. In this case, $2\pi l$ is the period of the plate temperature variations and ΔT is a characteristic temperature variation. At large distances from the plate the fluid flow is static and the temperature of the fluid remains at the uniform temperature T_∞. Cartesian coordinates $(\bar{x}, \bar{y})$ are chosen along and normal to the plate, respectively, and the fluid flow is assumed to be periodic in the $\bar{x}$-direction with the period $2\pi l$. We define the dimensionless variables as follows:

$$\begin{aligned} &t = (\alpha/l^2)\bar{t}, \quad x = \bar{x}/l, \quad y = \bar{y}/l, \\ &u = (l/\alpha)\bar{u}, \quad v = (l/\alpha)\bar{v}, \\ &\psi = \bar{\psi}/\alpha, \quad \omega = (l^2/\alpha)\bar{\omega}, \quad T = (\bar{T} - T_\infty)/\Delta T, \end{aligned} \tag{2}$$

where α is the thermal diffusivity, t the time, u and v are the velocity components in the x and y directions, respectively, T is the temperature, ω the vorticity and ψ is the stream function defined in the usual way, namely $u = \partial\psi/\partial y$ and $v = -\partial\psi/\partial x$. Under the Boussinesq approximation, the governing equations can be written in non-dimensional form as follows:

$$\nabla^2\psi = -\omega, \tag{3}$$

$$\frac{\partial\omega}{\partial t} + \frac{\partial\psi}{\partial y}\frac{\partial\omega}{\partial x} - \frac{\partial\psi}{\partial x}\frac{\partial\omega}{\partial y} = Pr\,\nabla^2\omega + Gr\,Pr^2\frac{\partial T}{\partial y}, \tag{4}$$

$$\frac{\partial T}{\partial t} + \frac{\partial\psi}{\partial y}\frac{\partial T}{\partial x} - \frac{\partial\psi}{\partial x}\frac{\partial T}{\partial y} = \nabla^2 T, \tag{5}$$

where ∇^2 is the Laplacian operator in the (x, y) coordinates, and Gr and Pr are the Grashof and the Prandtl numbers, respectively.

In addition to the periodic boundary conditions in x, on the plate the fluid velocity is zero and the temperature as prescribed by Eq. (1) become in non-dimensional form,

$$\psi = \frac{\partial\psi}{\partial y} = 0, \quad T = \sin x \quad \text{on } y = 0, \quad 0 \leqslant x \leqslant 2\pi. \tag{6}$$

Further, at large distances from the plate the fluid velocity is zero and the temperature is ambient and hence the boundary conditions are given by

$$\omega \to 0, \quad \frac{\partial\psi}{\partial y} \to 0, \quad T \to 0 \quad \text{as } y \to \infty, \quad 0 \leqslant x \leqslant 2\pi. \tag{7}$$

We have numerically solved the governing equations (3)–(5) using an unsteady approach although in this paper we are only interested in the steady state results. We have found that the unsteady numerical procedure employed can achieve the steady state solution much more rapidly than when using an iterative approach to the steady equations for large values of Gr.

In order to analyze the solutions for small values of the Grashof number, we introduce the following dimensionless variables

$$\tilde{t} = (U_0/l)\bar{t}, \quad x = \bar{x}/l, \quad y = \bar{y}/l,$$
$$\tilde{u} = \bar{u}/U_0, \quad \tilde{v} = \bar{v}/U_0,$$
$$\tilde{\psi} = \left(\frac{1}{U_0 l}\right)\bar{\psi}, \quad \tilde{\omega} = (l/U_0)\bar{\omega}, \quad \tilde{T} = (\bar{T} - T_\infty)/\Delta T, \tag{8}$$

where $U_0 = (g\beta\Delta T l)^{1/2}$ is the fluid velocity scaling. The relation between the scalings (2) and (8) is $t = 1/(Pr\,Gr^{1/2})\tilde{t}$, $\omega = Pr\,Gr^{1/2}\tilde{\omega}$, $\psi = Pr\,Gr^{1/2}\tilde{\psi}$ and $T = \tilde{T}$. Thus an alternative dimensionless form of the governing equations may be written as follows:

$$\nabla^2\tilde{\psi} = -\tilde{\omega}, \tag{9}$$

$$\frac{\partial\tilde{\omega}}{\partial\tilde{t}} + \frac{\partial\tilde{\psi}}{\partial y}\frac{\partial\tilde{\omega}}{\partial x} - \frac{\partial\tilde{\psi}}{\partial x}\frac{\partial\tilde{\omega}}{\partial y} = \frac{1}{Gr^{1/2}}\nabla^2\tilde{\omega} + \frac{\partial\tilde{T}}{\partial y}, \tag{10}$$

$$\frac{\partial\tilde{T}}{\partial\tilde{t}} + \frac{\partial\tilde{\psi}}{\partial y}\frac{\partial\tilde{T}}{\partial x} - \frac{\partial\tilde{\psi}}{\partial x}\frac{\partial\tilde{T}}{\partial y} = \frac{1}{Pr\,Gr^{1/2}}\nabla^2\tilde{T}, \tag{11}$$

and the boundary conditions for $\tilde{\omega}$, $\tilde{\psi}$ and $\tilde{T}$ are exactly same as those for ω, ψ and T, namely,

$$\tilde{\omega}, \tilde{\psi}, \tilde{T} \text{ are periodic functions of period } 2\pi \text{ in } x, \quad 0 \leqslant y < \infty,$$
$$\tilde{\psi} = \frac{\partial\tilde{\psi}}{\partial y} = 0, \quad \tilde{T} = \sin x \quad \text{on } y = 0, \quad 0 \leqslant x \leqslant 2\pi,$$
$$\tilde{\omega} \to 0, \quad \frac{\partial\tilde{\psi}}{\partial y} \to 0, \quad \tilde{T} \to 0 \quad \text{as } y \to \infty, \quad 0 \leqslant x \leqslant 2\pi. \tag{12}$$

For the steady problem, the governing equations are obtained by setting $\partial\tilde{\omega}/\partial\tilde{t} \equiv 0$ and $\partial\tilde{T}/\partial\tilde{t} \equiv 0$ in Eqs. (9)–(11), and we obtain the following equations:

$$\nabla^2\tilde{\psi} = -\tilde{\omega}, \tag{13}$$

$$\frac{\partial\tilde{\psi}}{\partial y}\frac{\partial\tilde{\omega}}{\partial x} - \frac{\partial\tilde{\psi}}{\partial x}\frac{\partial\tilde{\omega}}{\partial y} = \frac{1}{Gr^{1/2}}\nabla^2\tilde{\omega} + \frac{\partial\tilde{T}}{\partial y}, \tag{14}$$

$$\frac{\partial\tilde{\psi}}{\partial y}\frac{\partial\tilde{T}}{\partial x} - \frac{\partial\tilde{\psi}}{\partial x}\frac{\partial\tilde{T}}{\partial y} = \frac{1}{Pr\,Gr^{1/2}}\nabla^2\tilde{T}. \tag{15}$$

We use the governing equations in the form (13)–(15) in order to determine the asymptotic solution for small values of Gr and to construct the steady state numerical scheme.

3. Asymptotic solution of the steady problem for small values of *Gr*

In this section, we look for the perturbation solutions of Eqs. (13)–(15), subject to the boundary conditions (12), for small values of Gr. We assume that $\tilde{\omega}, \tilde{\psi}$ and $\tilde{T}$ may be expanded in powers of $Gr^{1/2}$ in the following form:

$$\begin{aligned}
\tilde{\omega} &= \omega_0 + Gr^{1/2}\omega_1 + Gr\omega_2 + Gr^{\frac{3}{2}}\omega_3 + Gr^2\omega_4 + \cdots,\\
\tilde{\psi} &= \psi_0 + Gr^{1/2}\psi_1 + Gr\psi_2 + Gr^{3/2}\psi_3 + Gr^2\psi_4 + \cdots,\\
\tilde{T} &= T_0 + Gr^{1/2}T_1 + GrT_2 + Gr^{3/2}T_3 + Gr^2T_4 + Gr^{5/2}T_5 + \cdots
\end{aligned} \tag{16}$$

On substitution of the series (16) into Eqs. (13)–(15), and collecting up terms of the same power of the Grashof number, we obtain the following sets of partial differential equations:

$$\nabla^2\omega_0 = 0, \quad \nabla^2\psi_0 = -\omega_0, \quad \nabla^2 T_0 = 0, \tag{17}$$

$$\begin{cases}
\nabla^2\omega_k + \frac{\partial T_{k-1}}{\partial y} = \sum_{m=0}^{k-1}\left(\frac{\partial\psi_m}{\partial y}\frac{\partial\omega_{k-m-1}}{\partial x} - \frac{\partial\psi_m}{\partial x}\frac{\partial\omega_{k-m-1}}{\partial y}\right),\\
\nabla^2\psi_k = -\omega_k,\\
\nabla^2 T_k = P_r\sum_{m=0}^{k-1}\left(\frac{\partial\psi_m}{\partial y}\frac{\partial T_{k-m-1}}{\partial x} - \frac{\partial\psi_m}{\partial x}\frac{\partial T_{k-m-1}}{\partial y}\right),
\end{cases} \tag{18}$$

where ω_k, ψ_k $(k = 0, 1, 2, \ldots)$ and T_0 have the same boundary conditions as $\tilde{\omega}, \tilde{\psi}$ and $\tilde{T}$, while T_k have the same boundary conditions as $\tilde{T}$ except that $T_k|_{y=0} = 0$ for $k = 1, 2, \ldots$. By solving these equations up to the fourth-order, we obtain closed form analytical solutions with Pr as an arbitrary parameter as follows:

$$\begin{aligned}
&\omega_0 = \psi_0 = 0, \quad T_0 = e^{-y}\sin x,\\
&\omega_1 = \left(\frac{1}{4} - \frac{1}{2}y\right)e^{-y}\sin x, \quad \psi_1 = -\frac{1}{8}y^2e^{-y}\sin x, \quad T_1 = 0,\\
&\omega_2 = \psi_2 = 0, \quad T_2 = Pr\left(\frac{1}{128}y + \frac{1}{64}y^2\right)e^{-2y}\sin 2x,\\
&\omega_3 = \left[-\frac{1}{4096}(1+Pr) + \frac{1}{1024}(1+2Pr)y + \frac{1}{512}y^2 - \frac{1}{384}(1+Pr)y^3\right]e^{-2y}\sin 2x,\\
&\psi_3 = \left[\frac{1}{8192}(1+Pr)y^2 - \frac{1}{6144}Pry^3 - \frac{1}{6144}(1+Pr)y^4\right]\times e^{-2y}\sin 2x, \quad T_3 = 0, \quad \omega_4 = \psi_4 = 0,\\
&T_4 = Pr\left\{\frac{1}{131\,072}(51Pr-6)e^{-y} + \left[\frac{1}{131\,072}(6-51Pr) + \frac{1}{32\,768}(3-28Pr)y + \frac{1}{32\,768}(3-33Pr)y^2 + \frac{1}{24\,576}(2-21Pr)y^3 + \frac{1}{24\,576}(1-11Pr)y^4\right]e^{-3y}\right\}\sin x\\
&\quad + Pr\left[-\frac{1}{2\,654\,208}(5-61Pr)y - \frac{1}{884\,736}(5-61Pr)y^2 + \frac{1}{221\,184}(2+35Pr)y^3 + \frac{1}{73\,728}(1+7Pr)y^4\right]e^{-3y}\sin 3x,\\
&T_5 = 0.
\end{aligned} \tag{19}$$

The structure of the above solution suggests that the full numerical solution at a finite value of the Grashof number may be expressed in the form of a Fourier series.

4. Full numerical method for the steady problem

Since $\tilde{\omega}, \tilde{\psi}$ and $\tilde{T}$ in Eqs. (13)–(15) are periodic functions of period 2π in the x direction, then this suggests that these functions have Fourier series expansions in x of the following form:

$$\begin{aligned}
\tilde{\omega}(x,y) &= \frac{1}{2}G_0(y) + \sum_{n=1}^{\infty}\{G_n(y)\cos nx + g_n(y)\sin nx\},\\
\tilde{\psi}(x,y) &= \frac{1}{2}F_0(y) + \sum_{n=1}^{\infty}\{F_n(y)\cos nx + f_n(y)\sin nx\},\\
\tilde{T}(x,y) &= \frac{1}{2}T_0(y) + \sum_{n=1}^{\infty}\{T_n(y)\cos nx + t_n(y)\sin nx\}.
\end{aligned} \tag{20}$$

By substituting the series (20) into Eqs. (13)–(15), multiplying by $1, \cos nx$ and $\sin nx$, respectively, and integrating from 0 to 2π with respect to x, we obtain the following system of ordinary differential equations:

$$\begin{aligned}
&\frac{1}{Gr^{1/2}}G_0'' = R_0 - T_0',\\
&\frac{1}{Gr^{1/2}}(G_n'' - n^2G_n) + \frac{1}{2}nf_{2n}'G_n + nf_{2n}G_n' = R_n - T_n',\\
&\frac{1}{Gr^{1/2}}(g_n'' - n^2g_n) - \frac{1}{2}nf_{2n}'g_n - nf_{2n}g_n' = r_n - t_n',\\
&F_0'' = -G_0, \quad F_n'' - n^2F_n = -G_n,\\
&f_n'' - n^2f_n = -g_n, \quad \frac{1}{Pr\,Gr^{1/2}}T_0'' = S_0,\\
&\frac{1}{Pr\,Gr^{1/2}}(T_n'' - n^2T_n) + \frac{1}{2}nf_{2n}'T_n + nf_{2n}T_n' = S_n,\\
&\frac{1}{Pr\,Gr^{1/2}}(t_n'' - n^2t_n) - \frac{1}{2}nf_{2n}'t_n - nf_{2n}t_n' = s_n,
\end{aligned} \tag{21}$$

where $n = 1, 2, \ldots,$ and

$$\begin{aligned}
R_0 &= \sum_{m=1}^{\infty} m(g_mF_m' - G_mf_m' - f_mG_m' + g_m'F_m),\\
R_n &= -\frac{1}{2}nf_nG_0' + \frac{1}{2}\sum_{m=1}^{\infty}\{[(m-n)F_{|m-n|} + (m+n)F_{m+n}]g_m'\\
&\quad + m(F_{|m-n|}' + F_{m+n}')g_m\} - \frac{1}{2}\sum_{m=1,m\neq n}^{\infty}\{[|m-n|f_{|m-n|}\\
&\quad + (m+n)f_{m+n}]G_m' + m[\mathrm{sgn}(m-n)f_{|m-n|}' + f_{m+n}']G_m\},\\
r_n &= \frac{1}{2}nF_nG_0' + \frac{1}{2}\sum_{m=1,m\neq n}^{\infty}\{[(m+n)f_{m+n} - |m-n|f_{|m-n|}]g_m'\\
&\quad - m[\mathrm{sgn}(m-n)f_{|m-n|}' - f_{m+n}']g_m\} - \frac{1}{2}\sum_{m=1}^{\infty}\{[(m-n)F_{|m-n|}\\
&\quad - (m+n)F_{m+n}]G_m' + m(F_{|m-n|}' - F_{m+n}')G_m\},\\
S_0 &= \sum_{m=1}^{\infty} m(t_mF_m' - T_mf_m' - f_mT_m' + t_m'F_m),\\
S_n &= -\frac{1}{2}nf_nT_0' + \frac{1}{2}\sum_{m=1}^{\infty}\{[(m-n)F_{|m-n|} + (m+n)F_{m+n}]t_m'\\
&\quad + m(F_{|m-n|}' + F_{m+n}')t_m\} - \frac{1}{2}\sum_{m=1,m\neq n}^{\infty}\{[|m-n|f_{|m-n|}\\
&\quad + (m+n)f_{m+n}]T_m' + m[\mathrm{sgn}(m-n)f_{|m-n|}' + f_{m+n}']T_m\},\\
s_n &= \frac{1}{2}nF_nT_0' + \frac{1}{2}\sum_{m=1,m\neq n}^{\infty}\{[(m+n)f_{m+n} - |m-n|f_{|m-n|}]t_m'\\
&\quad - m[\mathrm{sgn}(m-n)f_{|m-n|}' - f_{m+n}']t_m\} - \frac{1}{2}\sum_{m=1}^{\infty}\{[(m-n)F_{|m-n|}\\
&\quad - (m+n)F_{m+n}]T_m' + m(F_{|m-n|}' - F_{m+n}')T_m\}.
\end{aligned} \tag{22}$$

Here, primes denote differentiation with respect to y and $\mathrm{sgn}(m-n)$ means the sign of $(m-n)$ with $\mathrm{sgn}(0) = 0$. The boundary conditions (11) become

$$\begin{aligned}
&F_0(0) = F_0'(0) = 0, \quad T_0(0) = 0,\\
&F_n(0) = F_n'(0) = f_n(0) = f_n'(0) = 0,\\
&T_n(0) = 0, \quad t_n(0) = \delta_n,\\
&G_0 \to 0, \quad G_n \to 0, \quad g_n \to 0 \quad \text{as } y \to \infty,\\
&F_0' \to 0, \quad F_n' \to 0, \quad f_n' \to 0 \quad \text{as } y \to \infty,\\
&T_0 \to 0, \quad T_n \to 0, \quad t_n \to 0 \quad \text{as } y \to \infty,
\end{aligned} \tag{23}$$

where $n = 1, 2, 3, \ldots,$ $\delta_1 = 1$ and $\delta_n = 0$ $(n = 2, 3, \ldots)$. Here we only describe in detail how to solve the equations for g_n, f_n and t_n, but the equations for G_n, F_n and T_n can be solved in a similar manner. The iterative procedure is as follows:

$$\begin{aligned}
&\frac{1}{Gr^{1/2}}\left[(g_n^{(k+1)})'' - n^2g_n^{(k+1)}\right]\\
&\quad - \frac{1}{2}n(f_{2n}^k)'g_n^{(k+1)} - nf_{2n}^k(g_n^{(k+1)})' = r_n^k - (t_n^k)',\\
&(f_n^{(k+1)})'' - n^2f_n^{(k+1)} = -g_n^{(k+1)}, \quad f_n(0) = f_n'(0) = 0,\\
&g_n \to 0, \quad f_n' \to 0 \quad \text{as } y \to \infty,
\end{aligned} \tag{24}$$

$$\begin{aligned}
&\frac{1}{Pr\,Gr^{1/2}}[(t_n^{(k+1)})'' - n^2t_n^{(k+1)}] - \frac{1}{2}n(f_{2n}^k)'t_n^{(k+1)}\\
&\quad - nf_{2n}^k(t_n^{(k+1)})' = s_n^k,\\
&t_n(0) = \delta_n \qquad t_n \to 0 \quad \text{as } y \to \infty,
\end{aligned} \tag{25}$$

where k denotes the kth iteration. In order to overcome the lack of a vorticity boundary condition on $y = 0$, we use the same method as that described by Li [22]. The idea is to decompose the problem (24) into two problems. First, we solve the following problem:

$$\begin{aligned}
&\frac{1}{Gr^{1/2}}\left[(g_{1,n}^{(k+1)})'' - n^2 g_{1,n}^{(k+1)}\right] - \frac{1}{2}n(f_{2n}^{k})' g_{1,n}^{(k+1)} \\
&\quad - nf_{2n}^{k}(g_{1,n}^{(k+1)})' = r_n^k - (t_n^k)', \\
&(f_{1,n}^{(k+1)})'' - n^2 f_{1,n}^{(k+1)} = -g_{1,n}^{(k+1)}, \\
&g_{1,n}^{(k+1)}(0) = g_n^k(0), \quad g_{1,n}^{(k+1)} \to 0 \quad \text{as } y \to \infty, \\
&f_{1,n}^{(k+1)}(0) = 0, \quad (f_{1,n}^{(k+1)})' \to 0 \quad \text{as } y \to \infty.
\end{aligned} \tag{26}$$

and this is followed by the correction problem:

$$\begin{aligned}
&\frac{1}{Gr^{1/2}}\left[(g_{2,n}^{(k+1)})'' - n^2 g_{2,n}^{(k+1)}\right] - \frac{1}{2}n(f_{2n}^{k})' g_{2,n}^{(k+1)} \\
&\quad - nf_{2n}^{k}(g_{2,n}^{(k+1)})' = 0, \\
&(f_{2,n}^{(k+1)})'' - n^2 f_{2,n}^{(k+1)} = -g_{2,n}^{(k+1)}, \\
&g_{2,n}^{(k+1)} \to 0 \quad \text{as } y \to \infty, \\
&f_{2,n}^{(k+1)}(0) = 0, \quad (f_{2,n}^{(k+1)}(0))' = -(f_{1,n}^{(k+1)}(0))', \\
&(f_{2,n}^{(k+1)})' \to 0 \quad \text{as } y \to \infty.
\end{aligned} \tag{27}$$

Then the $(k+1)$th iterative solution for the problem (24) is defined by

$$g_n^{(k+1)} = g_{1,n}^{(k+1)} + g_{2,n}^{(k+1)}, \quad f_n^{(k+1)} = f_{1,n}^{(k+1)} + f_{2,n}^{(k+1)} \tag{28}$$

and g_n^{k+1} and f_n^{k+1} satisfy exactly the boundary conditions of the problem (24). It should be noted that the governing equations of the problem (27), and the boundary conditions $g_{*,n}^{k+1}(0) = 1, f_{*,n}^{k+1}(0) = 0, g_{*,n}^{k+1}(\infty) \to 0$ and $(f_{*,n}^{k+1})'(\infty) \to 0$, determine the solutions $g_{*,n}^{k+1}$ and $f_{*,n}^{k+1}$. Then $cg_{*,n}^{k+1}$ and $cf_{*,n}^{k+1}$ are the solutions of the problem (27), where c is determined from the condition that $c(f_{*,n}^{k+1}(0))' = -(f_{1,n}^{k+1}(0))'$. If the iterative procedure is convergent then we have $c = [g_n^{k+1}(0) - g_n^k(0)] \to 0$, i.e., the solution of the problem (27) tends to zero.

In our computations we have adopted the following transformations for the variable y:

$$\begin{aligned}
&z = \mathrm{e}^{-\gamma y} : y \in (0, y_1) \to z \in (z_1, 1), \\
&\eta = \frac{1}{1 + d(y - y_0)} : y \in (y_0, \infty) \to \eta \in (0, 1),
\end{aligned} \tag{29}$$

where $y_0 < y_1$ and d and γ are constants to be specified. The advantage of using these transformations is that a fine mesh near the vertical plate is produced and it is in this region where more detail is required in order to better approximate the more rapid changes in all the quantities which we are determining. Thus, we take the grid size $h_1 = 1/(M_1 + 1)$ for z and $z_1 = h_1$ and then $y_1 = -(1/\gamma)\ln h_1$. We discrete the equations with the variable z by using the central-difference approximations at $z = 2h_1, 3h_1, \ldots, M_1 h_1$. Next, we choose $y_0 = -(1/\gamma)\ln(2h_1)$. If $h_2 = 1/(M_2 + 1)$ is the grid size for η, we let $(1 - h_2) = 1/(1 + d(y_1 - y_0))$ and then we take $d = \gamma h_2/((1 - h_2)\ln 2)$. This means that we can use central differences at $\eta = 2h_2, 3h_2, \ldots, M_2 h_2$ for the equations with the variable η. At the first point $\eta = h_2$, the first derivative terms (for example, $2c^2\eta^3 g_n'$), which are introduced by transforming the second derivative term, are approximated by a forward-difference quotient and the other terms are approximated by central differences. Because of the relationship $\eta^3 = h_2^3$, the truncation error still remains $\mathrm{O}(h_2^2)$. The Neumann boundary conditions are approximated by the use of a second-order accurate formulae.

From the above method, the boundary conditions, and the expressions for R_0, R_n, S_0 and S_n, we observe that the numerical solution is anti-symmetrical if the initial iterative values are anti-symmetrical in x and we take these functional values to be those obtained from the previously obtained solutions at a lower value of Gr, starting with $Gr = 0$ (i.e. forced connection flow). This anti-symmetrical nature of the solutions is in agreement with the asymptotic solution of the steady problem for small values of Gr. We have successively found solutions for Grashof numbers 0, 100, 225, 400 and 625 and all the five numerical solutions retain the anti-symmetrical property. For $Gr = 400$ and $Gr = 625$, we change the iterative procedure, namely we use two sub-cycles to achieve the convergence of Eqs. (24) and (25). The first sub-cycle is to determine the vorticity and the stream function and the second sub-cycle is to determine the temperature function.

In all of the iterative procedures, under-relaxation is employed in order to obtain convergent solutions and we use ω_r to denote a relaxation parameter and ϵ as the criteria for the iterative procedure to converge. For example, we obtain $g_n^{(k+1)}$ from Eq. (28) if

$$|g_n^{(k+1)} - g_n^{(k)}| < \epsilon, \tag{30}$$

and then the iterative procedure is terminated, otherwise the new $(k+1)$th value which is introduced into the next iteration is given by

$$g_n^{(k+1)} = \omega_r g_n^{(k+1)} + (1 - \omega_r) g_n^{(k)}, \tag{31}$$

where $0 < \omega_r \leqslant 1$.

5. Numerical method for the quasi-steady problem

As for the steady problem, we assume that ω, ψ and T in Eqs. (3)–(5) have Fourier series expansions in x of the form:

$$\begin{aligned}
\omega(x,y,t) &= \frac{1}{2}G_0(y,t) + \sum_{n=1}^{\infty}\{G_n(y,t)\cos nx + g_n(y,t)\sin nx\}, \\
\psi(x,y,t) &= \frac{1}{2}F_0(y,t) + \sum_{n=1}^{\infty}\{F_n(y,t)\cos nx + f_n(y,t)\sin nx\}, \\
T(x,y,t) &= \frac{1}{2}T_0(y,t) + \sum_{n=1}^{\infty}\{T_n(y,t)\cos nx + t_n(y,t)\sin nx\},
\end{aligned} \tag{32}$$

where $G_0, F_0, T_0, G_n, F_n, T_n, g_n, f_n$ and t_n are given by the following equations:

$$\begin{aligned}
&\frac{\partial G_0}{\partial t} - Pr\frac{\partial^2 G_0}{\partial y^2} = GrPr^2\frac{\partial T_0}{\partial y} - R_0,\\
&\frac{\partial G_n}{\partial t} - Pr\left(\frac{\partial^2 G_n}{\partial y^2} - n^2 G_n\right) - \frac{1}{2}n\frac{\partial f_{2n}}{\partial y}G_n\\
&\quad - nf_{2n}\frac{\partial G_n}{\partial y} = GrPr^2\frac{\partial T_n}{\partial y} - R_n,\\
&\frac{\partial g_n}{\partial t} - Pr\left(\frac{\partial^2 g_n}{\partial y^2} - n^2 g_n\right) + \frac{1}{2}n\frac{\partial f_{2n}}{\partial y}g_n\\
&\quad + nf_{2n}\frac{\partial g_n}{\partial y} = GrPr^2\frac{\partial t_n}{\partial y} - r_n,\\
&\frac{\partial^2 F_0}{\partial y^2} = -G_0,\\
&\frac{\partial^2 F_n}{\partial y^2} - n^2 F_n = -G_n,\\
&\frac{\partial^2 f_n}{\partial y^2} - n^2 f_n = -g_n,\\
&\frac{\partial T_0}{\partial t} - \frac{\partial^2 T_0}{\partial y^2} = -S_0,\\
&\frac{\partial T_n}{\partial t} - \left(\frac{\partial^2 T_n}{\partial y^2} - n^2 T_n\right) - \frac{1}{2}n\frac{\partial f_{2n}}{\partial y}T_n - nf_{2n}\frac{\partial T_n}{\partial y} = -S_n,\\
&\frac{\partial t_n}{\partial t} - \left(\frac{\partial^2 t_n}{\partial y^2} - n^2 t_n\right) + \frac{1}{2}n\frac{\partial f_{2n}}{\partial y}t_n + nf_{2n}\frac{\partial t_n}{\partial y} = -s_n,
\end{aligned} \tag{33}$$

where $n = 1, 2, \ldots,$ $R_0, R_n, r_n, S_0, S_n, s_n$ and the boundary conditions are the same as those presented in Section 4, namely Eqs. (22) and (23). We now describe in detail how to solve the Eqs. (33) for g_n and f_n, while the other functions can be solved in a similar manner. On using the time step Δt, the equations for determining g_n and f_n are given by

$$\begin{aligned}
&\frac{g_n^{m+1} - g_n^m}{\Delta t} - \frac{1}{2}\left\{Pr\left[(g_n^{m+1})'' - n^2 g_n^{m+1}\right]\right.\\
&\quad \left. - \frac{1}{2}n(f_{2n}^{m+(1/2)})' g_n^{m+1} - nf_{2n}^{m+(1/2)}(g_n^{m+1})'\right\}\\
&= \frac{1}{2}\left\{Pr\left[(g_n^m)'' - n^2 g_n^m\right] - \frac{1}{2}n(f_{2n}^{m+(1/2)})' g_n^m\right.\\
&\quad \left. - nf_{2n}^{m+(1/2)}(g_n^m)'\right\} + GrPr^2(t_n^{m+(1/2)})' - r_n^{m+(1/2)},\\
&(f_n^{m+1})'' - n^2 f_n^{m+1} = -g_n^{m+1},\\
&f_n^{m+1}|_{y=0} = (f_n^{m+1})'|_{y=0} = 0,\\
&g_n^{m+1} \to 0, \quad (f_n^{m+1})' \to 0 \quad \text{as } y \to \infty,
\end{aligned} \tag{34}$$

where m denotes the mth level for the time step, $f_{2n}^{m+(1/2)} = (1/2)(f_{2n}^{m+1} + f_{2n}^m)$, etc. Eqs. (34) are solved by the same iterative technique as described in Section 4. Therefore we first consider the following problem:

$$\begin{aligned}
&g_{1,n}^{m+1} - \frac{\Delta t}{2}\left\{Pr\left[(g_{1,n}^{m+1})'' - n^2 g_{1,n}^{m+1}\right]\right.\\
&\quad \left. - \frac{1}{2}n(f_{2n}^{m+(1/2),k})' g_{1,n}^{m+1} - nf_{2n}^{m+(1/2),k}(g_{1,n}^{m+1})'\right\}\\
&= g_n^m + \frac{\Delta t}{2}\left\{Pr\left[(g_n^m)'' - n^2 g_n^m\right]\right.\\
&\quad \left. - \frac{1}{2}n(f_{2n}^{m+(1/2),k})' g_n^m - nf_{2n}^{m+(1/2),k}(g_n^m)'\right\}\\
&\quad + \Delta t\left[GrPr^2(t_n^{m+(1/2),k})' - r_n^{m+(1/2),k}\right],\\
&(f_{1,n}^{m+1})'' - n^2 f_{1,n}^{m+1} = -g_{1,n}^{m+1},\\
&g_{1,n}^{m+1}|_{y=0} = g_n^{m+1,k}|_{y=0}, \quad g_{1,n}^{m+1} \to 0 \quad \text{as } y \to \infty,\\
&f_{1,n}^{m+1}|_{y=0} = 0, \quad (f_{1,n}^{m+1})' \to 0 \quad \text{as } y \to \infty,
\end{aligned} \tag{35}$$

where the superscript k refers to the kth iteration, $f_{2n}^{m+(1/2),k} = (1/2)(f_{2n}^{m+1,k} + f_{2n}^m)$ and $g_n^{m+1,0}|_{y=0} = g_n^m|_{y=0}$. Next, we solve the following problem:

$$\begin{aligned}
&g_{2,n}^{m+1} - \frac{\Delta t}{2}\left\{Pr\left[(g_{2,n}^{m+1})'' - n^2 g_{2,n}^{m+1}\right]\right.\\
&\quad \left. - \frac{1}{2}n(f_{2n}^{m+(1/2),k})' g_{2,n}^{m+1} - nf_{2n}^{m+(1/2),k}(g_{2,n}^{m+1})'\right\} = 0,\\
&(f_{2,n}^{m+1})'' - n^2 f_{2,n}^{m+1} = -g_{2,n}^{m+1},\\
&g_{2,n}^{m+1} \to 0 \quad \text{as } y \to \infty,\\
&f_{2,n}^{m+1}(0) = 0,\\
&(f_{2,n}^{m+1}(0))' = -(f_{1,n}^{m+1}(0))', \quad (f_{2,n}^{m+1})' \to 0 \quad \text{as } y \to \infty.
\end{aligned} \tag{36}$$

At the $(m+1)$th time step, the $(k+1)$th iterative solutions for the problem (34) are defined by

$$g_n^{m+1,k+1} = g_{1,n}^{m+1} + g_{2,n}^{m+1}, \quad f_n^{m+1,k+1} = f_{1,n}^{m+1} + f_{2,n}^{m+1}. \tag{37}$$

We have $c = [g_n^{m+1,k+1}(0) - g_n^{m+1,k}(0)] \to 0$ if the iterative procedure is convergent. We also use the same variable transformations for y given by Eq. (29).

We start our calculations with the steady solution for $Gr = 100$ and then use these as the initial values when determining the solution for $Gr = 625$. We continue to use the solution obtained for the largest value of Gr for which we have a solution as the initial approximation for the solution at the next higher value of the Grashof number. Thus we find the steady state solutions using this approach for Grashof numbers 625–2500–5625–10 000. As in Section 4, we observe that the numerical solutions are anti-symmetrical if the initial values are anti-symmetrical and this is as we would have physically expected.

6. Numerical results and discussion

The asymptotic and numerical solutions have been computed for the steady problem (13)–(15) for small values of Gr. If we terminate the Fourier series after N terms then if N is sufficiently large then all the terms after the Nth term are extremely small. In our numerical procedure we have fixed a value of N and if the Nth term is sufficiently small, say less than 10^{-5} for the steady problem, then we have an accurate solution otherwise we choose a larger value of N and repeat the process. As a result, if Gr is small then the value of N can be taken to be small, for example, when $Gr \leqslant 225$ we have found that a value of $N = 20$ is sufficiently large. As the value of Gr increases then the value of N required to obtain accurate solutions also increases, for example, when $Gr = 10000$ then a value of $N = 48$ is necessary. In all the computations presented in this paper we have taken $Pr = 1$ but we have no difficulties in obtaining results for other O(1) values of Pr. Also we have found that a value of $\gamma = 0.5$, as introduced in the first variable transformation of y, see Eq. (29), is a reasonable value to take in order to achieve accurate results. When using the numerical method for the steady problem, results for

Table 1
The average Nusselt number $\overline{Nu}$

Gr	Asymptotic	$h_1 = 1/100$, $h_2 = 1/10$	$h_1 = 1/200$, $h_2 = 1/20$
0.01	2.00000	2.00000	2.00000
0.25	2.00001	2.00001	2.00001
1	2.00014	2.00014	2.00014
4	2.00222	2.00220	2.00221
9	2.01122	2.01097	2.01098
16	2.03546	2.03316	2.03318
25	2.08658	2.07445	2.07450
100	3.38522	2.48492	2.48522
225	9.01269	2.92087	2.92164
400	24.16355	3.30310	3.30459
625	56.11022	3.64491	3.64731

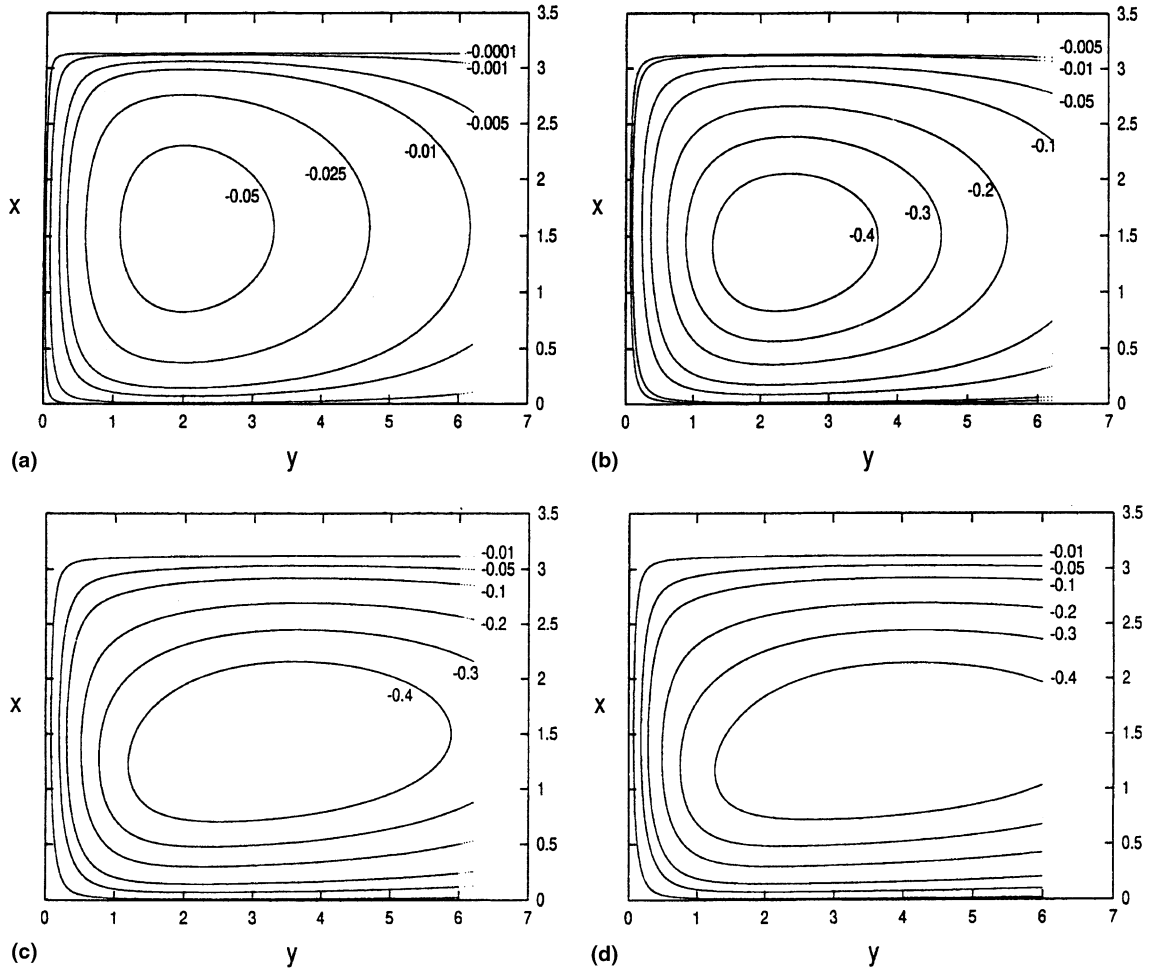

Fig. 1. The streamlines: (a) $Gr = 1$, (b) $Gr = 100$, (c) $Gr = 400$ and (d) $Gr = 625$ (steady and unsteady results).

$Gr \leqslant 225$ have been obtained using the grid sizes $h_1 = 1/100, h_2 = 1/10$ and $h_1 = 1/200, h_2 = 1/20$ and choosing $N = 20$, $\omega_r = 0.1$ and $\epsilon = 10^{-7}$ in the iterative procedures. However, for $Gr = 400$ and 625, the results obtained by using the steady numerical method were obtained with $N = 25$, $\omega_r = 0.1$ and $\epsilon = 10^{-6}$ and the sub-cycles technique has been employed in the iterative procedures.

The practical quantity of greatest interest is usually the average Nusselt number, $\overline{Nu}$, and it is given by

$$\overline{Nu} = -\int_0^{\pi} \frac{\partial T}{\partial y}\bigg|_{y=0} \mathrm{d}x. \tag{38}$$

We have computed the asymptotic solutions for small values of Gr, as given by Eqs (16), up to the $O(Gr^2)$ terms. By substitution of Eqs. (16) and (19) into Eq. (38), the asymptotic formula for the average Nusselt number $\overline{Nu}$ is given by

$$\overline{Nu} = 2 + \frac{1103}{7\ 962\ 624} Gr^2 + O(Gr^3). \tag{39}$$

The asymptotic and numerical results for the average Nusselt number are given in Table 1 for values of the Grashof number in the range 0.01–625. We see from Table 1 that the two sets of numerical results on different grids are in good agreement for all values of Gr up to 625. Also the numerical and asymptotic predictions are in very good agreement for $Gr \leqslant 4$. However, when $Gr = 25$, we observe that the error in the asymptotic solution is starting to become significant and this means that the asymptotic solution cannot be used for values of the Grashof numbers which are larger than about 25. It is seen from the results displayed in Table 1 how the heat transfer changes from being conduction dominated to the thermal boundary-layer convection situation.

Since the solutions are anti-symmetrical with respect to x, the streamlines and the isotherms are only shown

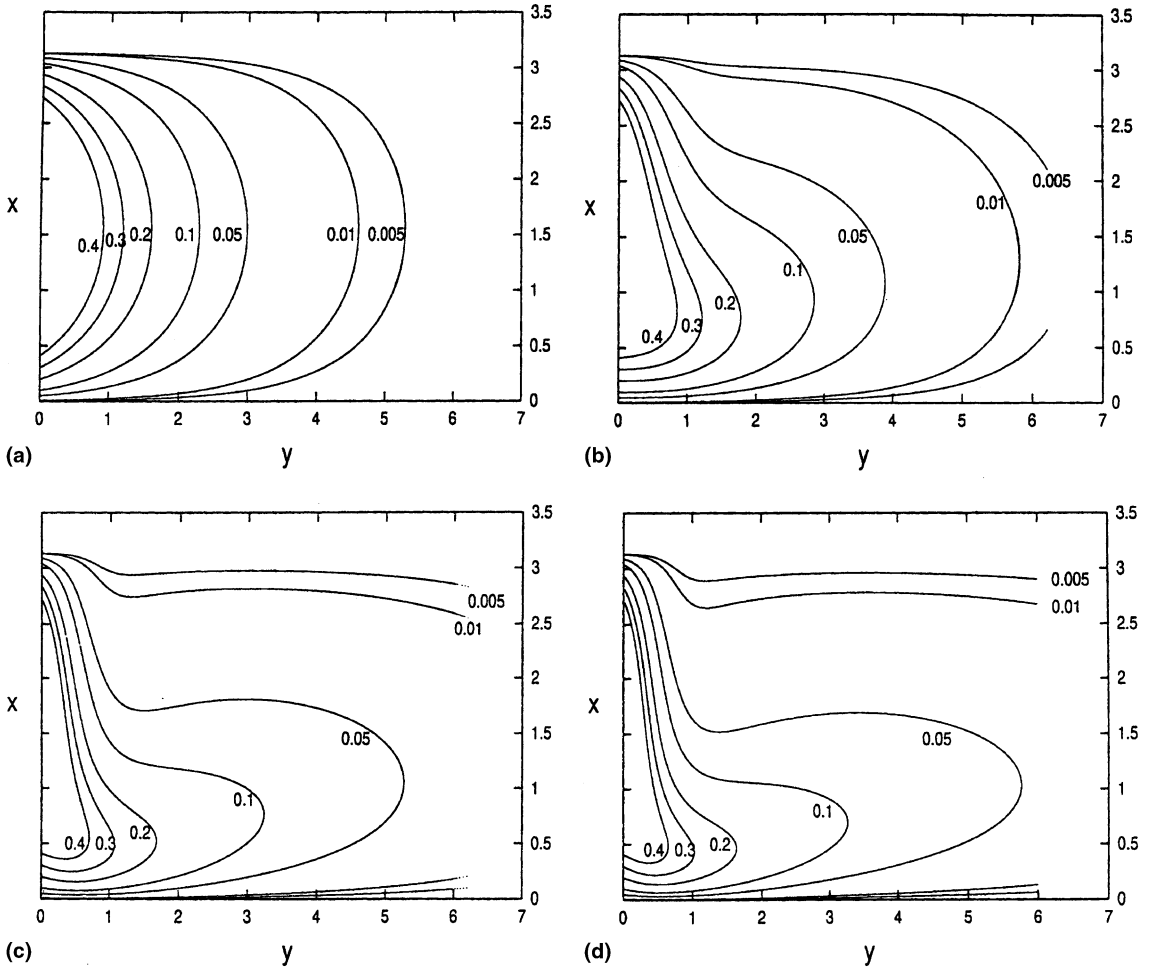

Fig. 2. The isotherms: (a) $Gr = 1$, (b) $Gr = 100$, (c) $Gr = 400$ and (d) $Gr = 625$ (steady and unsteady results).

on $[0,\pi]\times[0,2\pi]$ in Figs. 1 and 2 for $Gr = 1$, 100, 400 and 625. The results obtained from the two different grids employed are graphically indistinguishable and hence the results presented here are for the finer mesh. The streamline maps illustrated in Fig. 1 show that the heated flat plate generates a stream of fluid which flows upwards in the hot region near to the plate and this gives rise to a cellular motion. As we would physically expect, the distance that the cellular flow penetrates increases as Gr increases. Furthermore, these figures confirm that the oscillating wall temperature distribution induces a vertical boundary-layer flow that discharges itself horizontally into the surrounding fluid. On the other hand, we can see that the isotherms shown in Fig. 2(b) begin to distort and the distortion increases as the Grashof number increases.

For large values of the Grashof number, the solution of the steady equations using the iterative approach is not appropriate because of the huge amount of computational work that has to be performed. This is due to the use of the part explicit approximation for the convective terms in the series truncation method. Therefore we employ the unsteady numerical approach to obtain the steady solutions. In order to check the accuracy of the unsteady numerical solution approach, we compare the steady state results obtained from the unsteady numerical approach with the results obtained from the steady equations using an iterative process for $Gr = 625$. We have found that the unsteady solution rapidly approaches the steady solution if we numerically solve Eqs. (3)–(5). Further, it is important to note that in all the streamlines presented from the unsteady solutions, we have adopted the same scalings as those employed in the steady numerical solution approach. This means that if ψ is the numerical solution of Eqs. (3)–(5) then the values of $\psi/(PrGr^{1/2})$, which correspond to the scaling 8, are presented. At each time step under-relaxation is also adopted with $\omega_r = 0.1$, $\epsilon_1 = Gr^{1/2}\times 10^{-6}$ for the vorticity and the stream function and $\epsilon_2 = 10^{-6}$ for the temperature. The initial solution is taken to be the result obtained from the steady state approach with $Gr = 100$. The time steps are chosen to be $\Delta t = 0.0001$ for the first 10 steps, $\Delta t = 0.001$ for the 11–60th steps, $\Delta t = 0.005$ for the 61–80th steps, $\Delta t = 0.01$ for the 81–100th steps and $\Delta t = 0.05$ after the 100th step. Figs. 1(d) and 2(d) show the streamlines and the isotherms obtained from the steady and unsteady numerical solutions ($t = 7$) for $Gr = 625$. It is observed that the results obtained for the streamlines and the isotherms are indistinguishable from those obtained when using the steady state approach.

The average Nusselt number is shown in Fig 3 for $Gr = 625$ for $0 \leqslant t \leqslant 2$. We have found that at $t = 7$, the value of $\overline{Nu}$ is 3.64490 and this differs from the steady state value by only 0.00001. This confirms that the unsteady method gives very accurate solutions of the steady state problem. Fig. 3 also shows that, as expected,

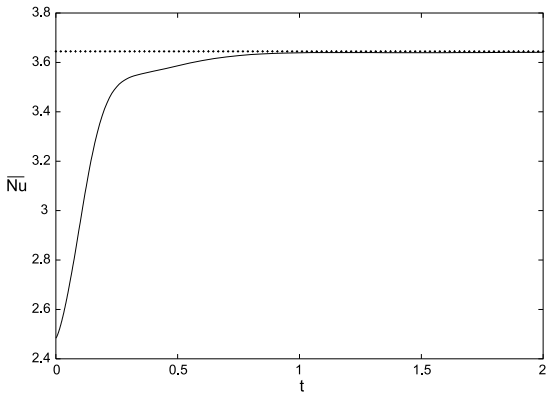

Fig. 3. The average Nusselt number as a function of the dimensionless time t for $Gr = 625$. $(+\,+\,+)$ steady result; $(-\,-\,-)$ unsteady result.

the average Nusselt number rapidly increases from its initial value to its final steady state value.

Using the unsteady numerical method, numerical results have also been obtained for $Gr = 2500, 5625,$ 10 000. In the computations we have taken $N = 32$ for $Gr = 2500$, $N = 40$ for $Gr = 5625$ and $N = 48$ for $Gr =$ 10 000 and the same grid size $h_1 = 1/100, h_2 = 1/10$ for the three values of Gr. The average Nusselt numbers are shown in Fig. 4 for $Gr = 2500$, 5625 and 10 000 as a function of time for $0 \leqslant t \leqslant 2$ and clearly there is a rapid approach to the steady state as time increases. At $t = 7$, the average Nusselt numbers are 5.00869, 6.06368 and 6.95319 for $Gr = 2500, 5625$ and 10 000, respectively. Figs. 5 and 6 show the streamlines and the isotherms at $t = 7$ for $Gr = 2500$ and 10 000 with $h_1 = 1/100, h_2 = 1/10$. We observe from these figures that the streamlines and the isotherms exhibit a similar form to those obtained from using the steady state equations, see Figs. 1 and 2. We observe that the flow consists of symmetrical

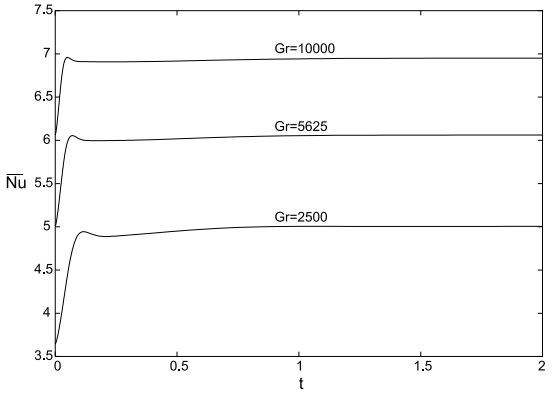

Fig. 4. The average Nusselt numbers for $Gr = 2500$, $Gr = 5625$ and $Gr = 10\,000$ as a function of the dimensionless time t.

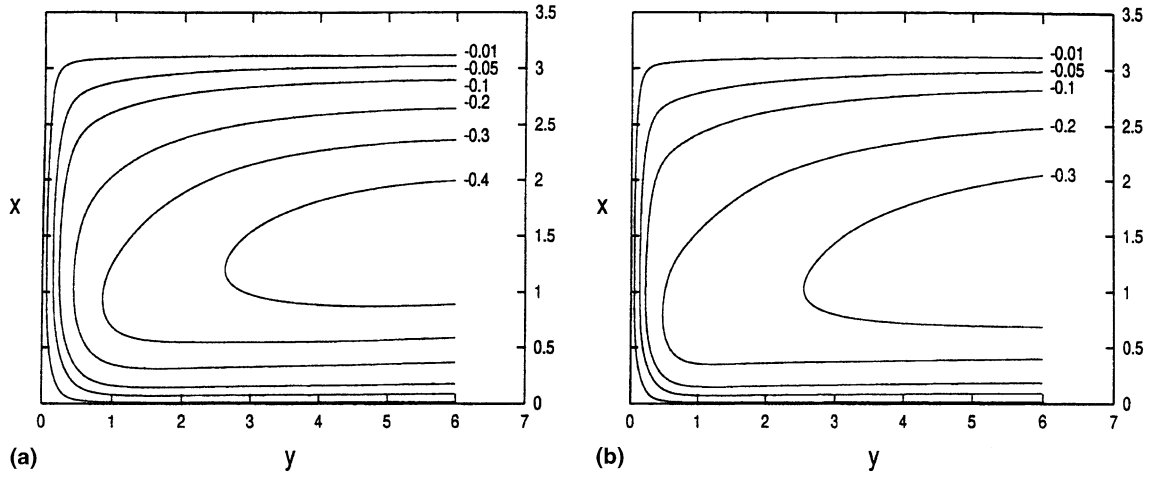

Fig. 5. The streamlines at the dimensionless time $t = 7$: (a) $Gr = 2500$ and (b) $Gr = 10000$.

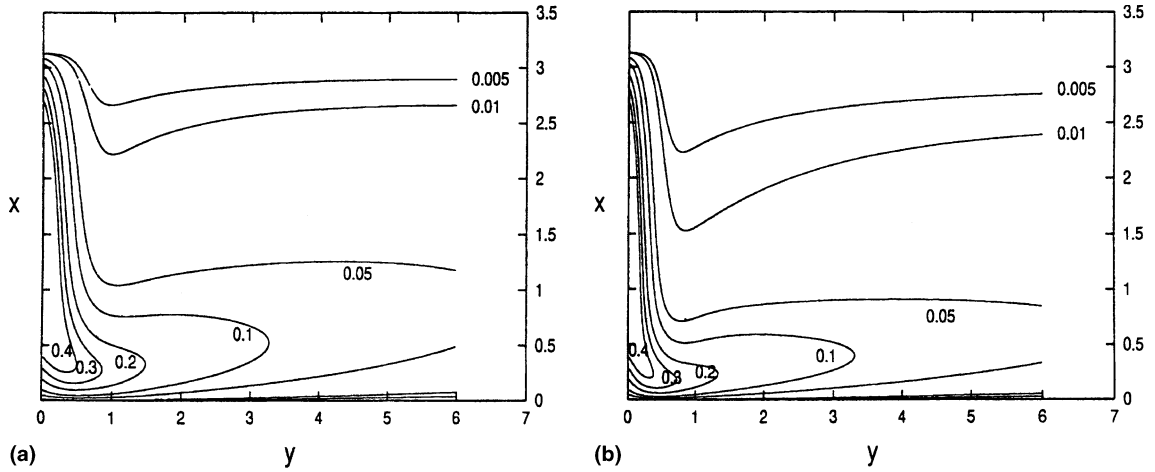

Fig. 6. The isotherms at the dimensionless time $t = 7$: (a) $Gr = 2500$ and (b) $Gr = 10000$.

cells whose relative size and shape depend on the Grashof number and have a significant effect on the heat transfer across the boundary-layer. Thus, all the results presented in this paper give us a good degree of confidence in the methods employed.

7. Conclusions

The steady and unsteady numerical methods for the natural convection flow from a vertical flat plate with a surface temperature oscillation have been investigated. For the steady problem with small values of the Grashof number, the asymptotic formula for the average Nusselt number is obtained by a perturbation method. The heat transfer occurs because of the oscillating wall temperature distributions and the average Nusselt number increases as the Grashof number increases. For small values of Gr, the heat and cellular flow penetrate into the surrounding fluid horizontally and smoothly and as the Grashof number increases then the temperatute distribution becomes more distortive. For very large values of Gr, up to 10 000, the flow remains steady and all the numerical results show that the proposed methods of solution are very efficient and accurate. These methods can easily be extended to other heat transfer problems.

Acknowledgements

This work was performed whilst Dr. Jian Li was visiting the Department of Applied Mathematics, University of Leeds and he was financially supported by the Royal Society China Royal Fellowship Scheme. He

would like to thank Drs. L. Elliott and X. Wen for all their kind assistance.

References

[1] E. Pohlhausen, Der wärmeaustausch zwischen festen körpen und flussigkeiten mit kleiner reibung und kleiner wärmeleitung, J. Appl. Math. Mech. (ZAMM) 1 (1921) 115–121.
[2] Y. Jaluria, Natural Convection: Heat and Mass Transfer, Pergamon Press, Oxford, 1980.
[3] Y. Jaluria, Basics of natural convection, in: S. Kakac, R.K. Shah, W. Aung (Eds.), Handbook of Single-Phase Convective Heat Transfer, Wiley, New York, 1987, pp. 12.1–12.31 (Chapter 12).
[4] B. Gebhart, Y. Jaluria, R.L. Mahajan, B. Samakia, Buoyancy Induced Flows and Transport, Hemisphere, New York, 1998.
[5] O.G. Martynenko, Yu.A. Sokovishin, Buoyancy-induced heat transfer on a vertical nonisothermal surface, in: O.G. Martynenko, A.A. Žukauskas (Eds.), Heat Transfer Soviet Reviews, vol. 1: Convective Heat Transfer, Hemisphere, New York, 1989, pp. 211–451.
[6] A. Bejan, Convection Heat Transfer, second ed., Wiley, New York, 1995.
[7] I. Pop, D.B. Ingham, J.H. Merkin, Transient convective heat transfer in external flow, in: P. Tyvand (Ed.), Advances in Fluid Mechanics, vol. 19: Time-dependent Nonlinear Convection, Computational Mechanics Publications, Southampton, 1998, pp. 83–114 (Chapter 3).
[8] I. Pop, D.B. Ingham, Convective Flows (in preparation).
[9] E.M. Sparrow, J.L. Gregg, Similar solutions for free convecton from a nonisothermal vertical plate, Trans. ASME J. Heat Transfer 80 (1958) 379–384.
[10] V.I. Semenov, Similar problems of steady-state laminar free convection on a vertical plate, Heat Transfer – Soviet Res. 16 (1984) 69–85.
[11] E.M. Sparrow, H. Quack, C.J. Boerner, Local non-similar boundary layer solutions, AIAA J. 8 (1970) 1936–1942.
[12] M. Keller, K.T. Yang, A Gőrtler-type series for laminar free convection along a non-isothermal vertical flat plate, Quart. J. Mech. Appl. Math. 25 (1972) 447–457.
[13] T.T. Kao, G.A. Domoto, H.G. Elrod Jr., Free convection along a nonisothermal vertical flat plate, Trans. ASME J. Heat Transfer 99 (1977) 72–78.
[14] J. Yang, D.R. Jeng, K.J. DeWitt, Laminar free convection from a vertical plate with nonuniform surface conditions, Numer. Heat Transfer 5 (1982) 165–184.
[15] H.J. Merk, Rapid calculation for boundary-layer transfer using wedge solutions and asymptotic expansions, J. Fluid Mech. 5 (1959) 460–480.
[16] T.Y. Na, Numerical solution of natural convection flow past a non-isothermal vertical flat plate, Appl. Scientific Res. 33 (1978) 519–543.
[17] H.B. Keller, T. Cebeci, Accurate numerical methods for boundary layer flows 1: two-dimensional flows, in: Proceedings of the International Conference on Numerical Methods in Fluid Dynamics, Lecture Notes in Physics, Springer, New York, 1971.
[18] T. Cebeci, P. Bradshaw, Physical and Computational Aspects of Convective Heat Transfer, Springer, New York, 1984.
[19] D.P. Telionis, Unsteady Viscous Flows, Springer, New York, 1981.
[20] T.T. Kao, Locally nonsimilar solution for laminar free convection adjacent to a vertical wall, Trans. ASME J. Heat Transfer 98 (1976) 321–322.
[21] D.A.S. Rees, The effect of steady streamwise surface temperature variations on vertical free convection, Int. J. Heat Mass Transfer 42 (1999) 2455–2464.
[22] J. Li, Correction methods for steady incompressible flows, J. Comput. Math. 17 (1999) 419–424.
[23] S.C.R. Dennis, G.-Z. Chang, Numerical solutions for steady flow past a circular cylinder at Reynolds numbers up to 100, J. Fluid Mech. 42 (1970) 471–489.
[24] W.M. Collins, S.C.R. Dennis, Flow past an impulsively started circular cylinder, J. Fluid Mech. 60 (1973) 105–127.
[25] D. Poulikakos, A. Bejan, Natural convection in a porous layer heated and cooled along one vertical side, Int. J. Heat Mass Transfer 27 (1984) 1879–1891.
[26] R. Bradean, D.B. Ingham, P.J. Heggs, I. Pop, Free convection fluid flow due to a periodically heated and cooled vertical flat plate embedded in a porous media, Int. J. Heat Mass Transfer 39 (1996) 2545–2557.
[27] R. Bradean, D.B. Ingham, P.J. Heggs, I. Pop, The unsteady penetration of free convection flows caused by heating and coolong flat surfaces in a porous media, Int. J. Heat Mass Transfer 40 (1997) 665–687.
[28] R. Bradean, P.J. Heggs, D.B. Ingham, I. Pop, Convective heat flow from suddenly heated surfaces embedded in porous media, in: D.B. Ingham, I. Pop (Eds.), Transport Phenomena in Porous Media, Pergamon Press, Oxford, 1998, pp. 411–438.
[29] D.A.S. Rees, Three-dimensional free convection boundary layers in porous media induced by a heated surface with spanwise temperature variations, Trans. ASME J. Heat Transfer 119 (1997) 792–798.